Chapter 5

Cation-π Interactions in the $GABA_A$ and Glycine Receptors Mediate Neurotransmitter Binding

Reproduced in part from:
Claire L. Padgett, A.P. Hanek, H.A. Lester, D.A. Dougherty, and Sarah C.R. Lummis;
J. Neurosci **2007**, 27 (4), 886-892

And

S.A. Pless, K.S. Millen, A.P. Hanek, J.W. Lynch, H.A. Lester, S.C.R. Lummis,
and D.A. Dougherty; *J. Neurosci* **2008** 28 (43), 10937-10942

5.1 Introduction

5.1.1 Cys-loop Neurotransmitter Gated Ion Channels

The γ-amino butyric acid type A ($GABA_A$) and glycine (Gly) receptors are members of the Cys-loop ligand-gated ion channel family, which also includes the nicotinic acetylcholine (nACh), serotonin type 3 ($5\text{-}HT_3$), and γ-amino butyric acid type C ($GABA_C$) receptors. These proteins mediate rapid synaptic transmission in the central and peripheral nervous systems. At rest the receptors are in a closed, non-conducting state. Upon binding of neurotransmitter, the receptor undergoes a conformational change to an open, ion-conducting state, thereby allowing ions to cross the cell membrane, converting a chemical signal (neurotransmitter) to an electrical one.

Each protein has five homologous subunits arranged pseudo-symmetrically around a central ion-conducting pore. Each subunit has a large extraceullular ligand-binding amino-terminal domain principally comprised of two beta sheets, four membrane-spanning helices (M1-M4), a large intracellular loop, and a short extracellular carboxy

tail. The beta strands in the extracellular domain are connected by short, unstructured loops which contribute to ligand binding and to transduction of the conformational change that takes place upon ligand binding.

Agonist binding sites are located at select subunit interfaces. The principle subunit contributes residues located on loops A, B, and C while the complementary subunit contributes loops D, E, and F. Of particular importance are a group of aromatic amino acids associated with loops A-D.[1] These aromatic residues are clustered together in a box-like structure (Figure 5.1) in the crystal structure of the acetylcholine binding protein (AChBP), which is homologous to the extraceullular domain of the $GABA_A$ and Gly receptors.[2] The resulting aromatic box is the location of cation-π interactions between acetylcholine and nicotine in the nAChR,[3,4] serotonin in the $5HT_{3A}R$ and MOD-1 receptor (Cys-loop receptor found in C. *elegans*),[5-7] and GABA in the $GABA_CR$ (Table 5.1).[8]

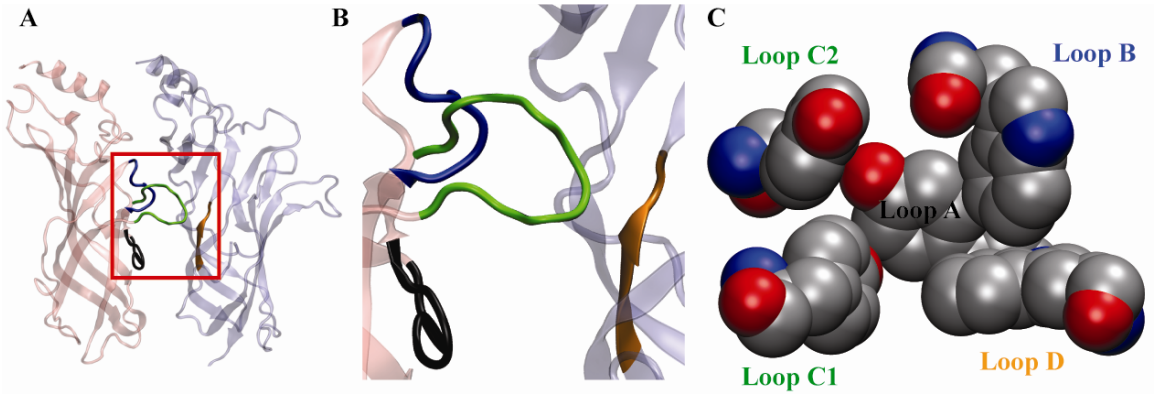

Figure 5.1 The ligand binding site of the nAChR. **A,** The agonist binding site is located at the interface between two subunits; the principle subunit is shown in pink and the complementary in gray. **B,** the area of **A** in the red box highlights the loops A (black), B (blue), and C (green) from the principle subunit and loop D (orange) from the complementary subunit. **C**, The aromatic box from the AChBP structure consists of a Tyr (loop A), Trp (loop B), two Tyr (loop C, residue 1 and 2), and Trp (loop D).

Cation-π interactions have been identified in the binding site of four members of the Cys-loop superfamily: muscle-type nAChR,[4] neuronal $\alpha_4\beta_2$ nAChR,[3] 5-$HT_{3A}R$,[5,6] and

$GABA_cR$.[8] Given the data on these other receptors, the high homology among the Cys-loop superfamily and especially the conservation of the aromatic box (Table 5.1), it seems reasonable that the other predominant mammalian inhibitory Cys-loop receptors, $GABA_AR$ and GlyR, will also bind neurotransmitter agonist through a cation-π interaction.

Table 5.1 The aromatic box is conserved across the Cys-loop family. Residues previously identified as participating in cation-π interactions are shown in red.

Receptor	A	B	C1	C2	D
nACh	Tyr	**Trp**	Tyr	Tyr	Trp
5-HT_3	Glu	**Trp**	Phe	Tyr	Tyr
$GABA_C$	Phe	**Tyr**	Tyr	Tyr	Tyr
$GABA_A$	Tyr	Tyr	Phe	Tyr	Phe
Gly	Phe	Phe	Tyr	Phe	Phe

5.1.2 The Binding Sites

The $\alpha_1\beta_2$ $GABA_AR$ studied has two binding sites, each located at a β/α interface. Given that $GABA_CR$ and $GABA_AR$ both bind GABA (structure, Figure 5.6) and that the aromatic boxes are highly similar (Table 5.1), it seems likely that GABA will bind in a similar manner, making the loop B residue (β_2Tyr157) the most likely candidate for the cation-π interaction. This seems especially likely since the residue is conserved as a Tyr. The other residues in the aromatic box (Figure 5.2) are β_2Tyr97 (loop A), β_2Phe200 (loop C1), β_2Tyr205 (loop C2), and α_1Phe65 (loop D).

The α_1 GlyR is homomeric, thus there are five possible binding sites. Unlike the other Cys-loop receptor binding sites, the predominant aromatic in the GlyR aromatic box is Phe (Figure 5.2, Table 5.1). This is especially intriguing given that no neurotransmitter-Cys-loop receptor cation-π interactions have been found at Phe sites.

Together, α_1Phe99 (loop A), α_1Phe159 (loop B), α_1Tyr202 (loop C1), α_1Phe207 (loop C2), and α_1Phe63 (loop D) comprise the aromatic box.

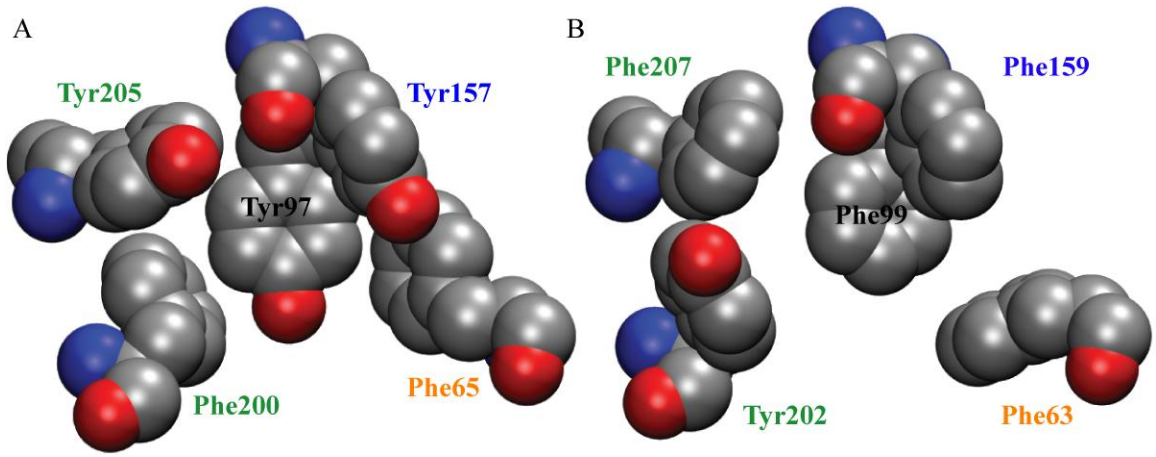

Figure 5.2 The aromatic box of the $GABA_AR$ (**A**) and GlyR (**B**), from homology models based on PDB structure 2BG9.

5.1.3 Probing Cys-loop Receptors for a Cation-π Interaction

Cation-π interactions can be identified by incorporation of fluorinated aromatics at prospective cation-π sites. The cation-π binding affinity of aromatics is strongly influenced by electrostatics, and addition of electron-withdrawing fluorines around the aromatic ring systematically diminishes the negative electrostatic potential on the face of the ring (Figure 5.3), and thus the cation-π binding ability.[9] Thus, a systematic increase in EC_{50} with increasing fluorination provides compelling evidence for a cation-π interaction. The reluctance to participate in H-bonding interactions and small steric size further make fluorine an ideal substituent. Here, we use a series of Phe analogs that contain an increasing number of fluorine atoms on their phenyl rings to probe potential cation-π interactions at the aromatic residues that contribute to the binding sites of the

$\alpha_1\beta_2$ $GABA_A$ and α_1 Gly receptors. These unnatural amino acids were incorporated into receptors expressed in Xenopus oocytes using nonsense suppression.[10,11]

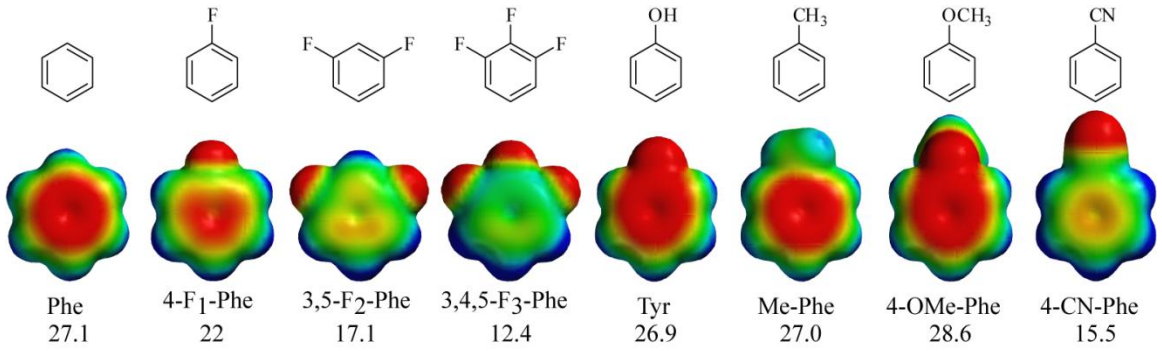

Figure 5.3 Electrostatic potential surfaces of phenylalanine analog side chains. All surfaces are scaled such that red is -40 kcal/mol and blue is +40 kcal/mol. The cation-π binding ability (calculated in the gas phase with a sodium ion using Hartree-Fock 6-31G** methods) is given below in kcal/mol.

5.2 Results

5.2.1 γ-Aminobutyric Acid Receptor

Probing of tryptophan and phenylalanine residues via successive fluorination is straightforward, whereas the 4-position hydroxyl group of tyrosine introduces a complication. Adding electron withdrawing groups to the phenyl ring of Tyr substantially lowers the pK_a of the hydroxyl, such that highly fluorinated tyrosines are expected to be ionized at physiological pH. To avoid complications from the ionization of tyrosines, we first study the Tyr to Phe mutant and then introduce fluorinated phenylalanines. Previous studies have validated this strategy.[8]

Mutation to Phe at $\beta_2$97 was well-tolerated, lowering the EC_{50} to 0.6 μM (Table 5.2). When referenced to the Phe mutation, introduction of a single fluorine increased the EC_{50} 33-fold. Incorporation of 3,5-F_2Phe and then 3,4,5-F_3Phe further increased the EC_{50} 700- and 16,500-fold, respectively, indicating a 22-fold and 24-fold increase for each additional fluorine, respectively. Hill coefficients and macroscopic currents did not

change appreciably. The systematic increase in EC_{50} with the addition of fluorines at position $\beta_2$97 indicates a cation-π interaction is present. The dose-response relationships and a fluorination plot[4] of the cation-π binding energy[9] and the EC_{50} values compared with the parent Phe are shown in Figure 5.4.

Table 5.2 EC_{50} values (μM) for incorporation of fluorinated Phe residues at β_2Tyr97

Amino Acid	EC_{50}	$EC_{50}/EC_{50(WT)}$	$EC_{50}/EC_{50(Phe)}$	n_H	N
$\alpha_1\beta_2$ (WT)	3.5	1	5.8	1.2	4
Phe	0.6	0.17	1	1.4	4
4-F_1Phe	20	5.7	33	1.2	5
3,5-F_2Phe	420	120	700	1.1	4
3,4,5-F_3Phe	9900	2800	16,500	1.9	5

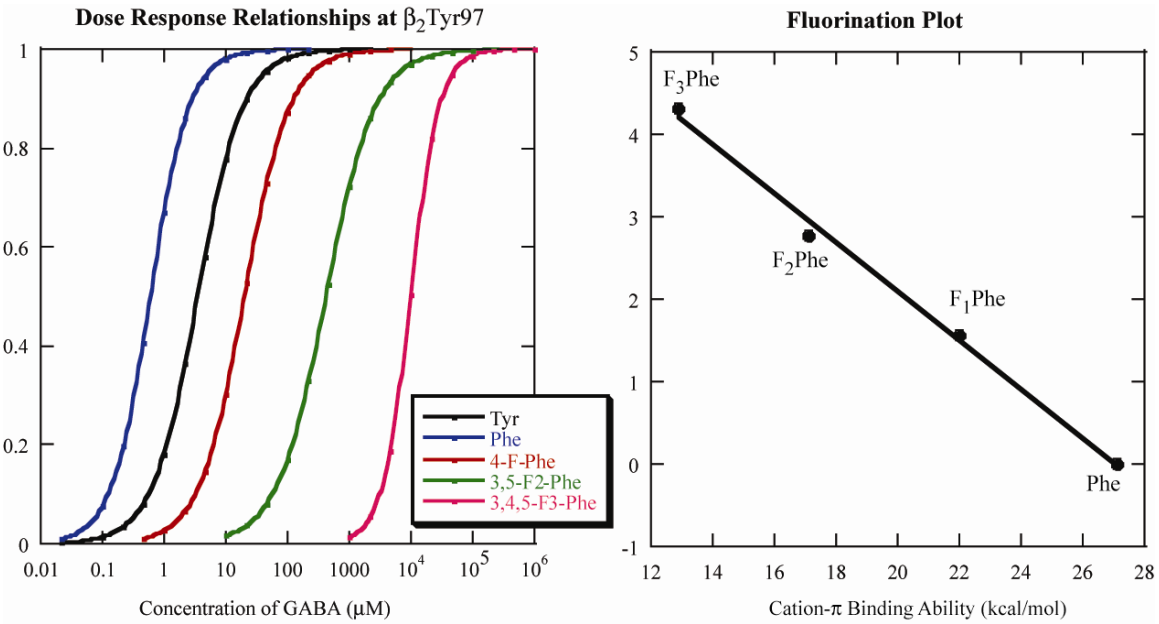

Figure 5.4 The dose response relationship shifts rightward with addition of fluorine residues (left panel). The fluorination plot (right panel) for Phe and Phe analogs at β_2Tyr97 of $GABA_AR$

The β_2Tyr157Phe mutation caused a 400-fold increase in the GABA EC_{50} to 1400 μM (Table 5.3), due to the removal of the 4 position hydroxyl. Incorporation of F_1Phe at the same position restored a wild type like $EC_{50,}$ while incorporation of 3,5-F_2Phe and 3,4,5-F_3Phe increased the EC_{50} but not in a manner consistent with a cation-π interaction.

The sensitivity of the receptor to the Phe mutation but not 4-F_1Phe strongly suggested the hydroxyl of tyrosine was important for channel function. To probe whether or not the OH group filled a steric or hydrogen bonding role, 4-Me-Phe and 4-OMe-Phe were incorporated. The 4-Me-Phe mutant has an EC_{50} 10-fold lower than the Phe mutant but 43-fold higher than wild type. 4-OMe-Phe, however, has an EC_{50} of 5 μM. Partial rescue of the Phe mutant by 4-Me-Phe suggests there is a steric component to the role of the 4 position hydroxyl at β_2Tyr157. Nearly full restoration of the wild type function by 4-OMe-Phe suggests that in addition to a steric role, the hydroxyl of β_2Tyr157 is a hydrogen bond acceptor.

Table 5.3 EC_{50} values for Phe analogues at β_2Tyr157 (loop B), β_2Tyr205 (loop C), and α_1Phe65 (loop D). EC_{50} values are given in μM; n_H is the hill coefficient; and N is the number of oocytes used.

β_2Tyr157	EC_{50}	n_H	N	β_2Tyr205	EC_{50}	n_H	N	α_1Phe65	EC_{50}	n_H	N
Phe	1400	0.9	6	Phe	80	1.4	5	Phe	3.0	1.2	4
F_1Phe	3.0	1.2	6	F_1Phe	1.5	1.9	3	F_1Phe	11	1.4	3
F_2Phe	420	2.0	4	F_2Phe	70	1.9	4				
F_3Phe	110	1.7	4	F_3Phe	90	2.5	4	F_3Phe	11.5	1.5	3
MePhe	5.0	1.2	3								
OMePhe	150	0.8	3								

Substitutions at position β_2Tyr205 (Table 5.3) showed some similarity to those at β_2Tyr157. There was an increase of 24-fold in EC_{50} for the Tyr to Phe mutation, but a wild-type EC_{50} for mutation to 4-F_1Phe. Incorporation of 3,5-F_2- or 3,4,5-F_3-Phe at this position yielded a similar EC_{50} to phenylalanine.

Incorporation of phenylalanine at the loop D residue, α_1Phe65, through nonsense suppression (wild type recovery) reproduced the wild-type GABA EC_{50} (Table 5.3). Addition of a fluorine to the phenyl ring increased EC_{50} to 11 μM. Incorporation of

F_3Phe did not further increase the EC_{50}. There were no significant differences in Hill coefficients for these mutations.

5.2.2 Glycine Results

An alignment of amino acid residues contributing to the aromatic box in Cys-loop receptors reveals that Phe63, Phe99, Phe159, Tyr202, and Phe207 of the α_1 GlyR are all possible candidates to contribute to a cation-π interaction (Table 5.1). A cation-π interaction at Phe99 or Tyr202 was ruled out on the basis of previous studies using conventional mutagenesis.[12,13] Therefore we selected Phe63, Phe159, and Phe 207 for unnatural amino acid incorporation. A recent study using conventional mutagenesis and a computational model[14] implicate Phe159 and Phe207 in a joint cation-π interaction with the glycine amino group (structure, Figure 5.6), making these two residues of particular interest.

Fluorinated Phe residues were incorporated using nonsense suppression. When coinjected with Phe-tRNA, mutant mRNAs encoding Phe63TAG, Phe159TAG, Phe207TAG, and Phe159TAG/Phe207TAG receptors produced functional receptors that responded to the application of glycine. Maximal currents (I_{max}), EC_{50} and n_H values were similar to each other, and to previously published results for wild-type (WT) α_1 homopentameric GlyRs expressed in *Xenopus* oocytes.[15] We thus conclude that the wild-type phenotype is successfully rescued by the nonsense suppression method.

Successive addition of fluorines to Phe159 leads to a progressive decrease in glycine sensitivity (Figure 5.5, Table 5.4), indicating a cation-π interaction at this site. 4-CN-Phe generates an EC_{50} value intermediate between those for 3,5-F_2Phe and 3,4,5-F_3Phe, as predicted by cation-π binding ability.[9] As in previous studies with Trp and Tyr,

the fluorination plot[4] demonstrates a strong linear correlation between the cation-π binding ability and relative log EC_{50} value (scaled to wild type). The magnitude and consistency of the effect show a significant cation-π interaction at Phe159.

Table 5.4 EC_{50} values (μM) for incorporation of fluorinated Phe residues at Phe159. I_{max} is reported in μA

Amino Acid	EC_{50}	$EC_{50}/EC_{50(Phe)}$	n_H	I_{max}	N
Phe	109 ± 2	1	2.8 ± 0.2	7.4 ± 0.6	5
4-F_1Phe	288 ± 6	2.6	3.1 ± 0.2	7 ± 1	4
3,5-F_2Phe	11000 ± 200	100	2.0 ± 0.1	7.7 ± 0.6	6
3,4,5-F_3Phe	103000 ± 3000	940	2.3 ± 0.1	5.6 ± 0.6	7
4-CN-Phe	46000 ± 1000	420	1.9 ± 0.1	9 ± 1	9

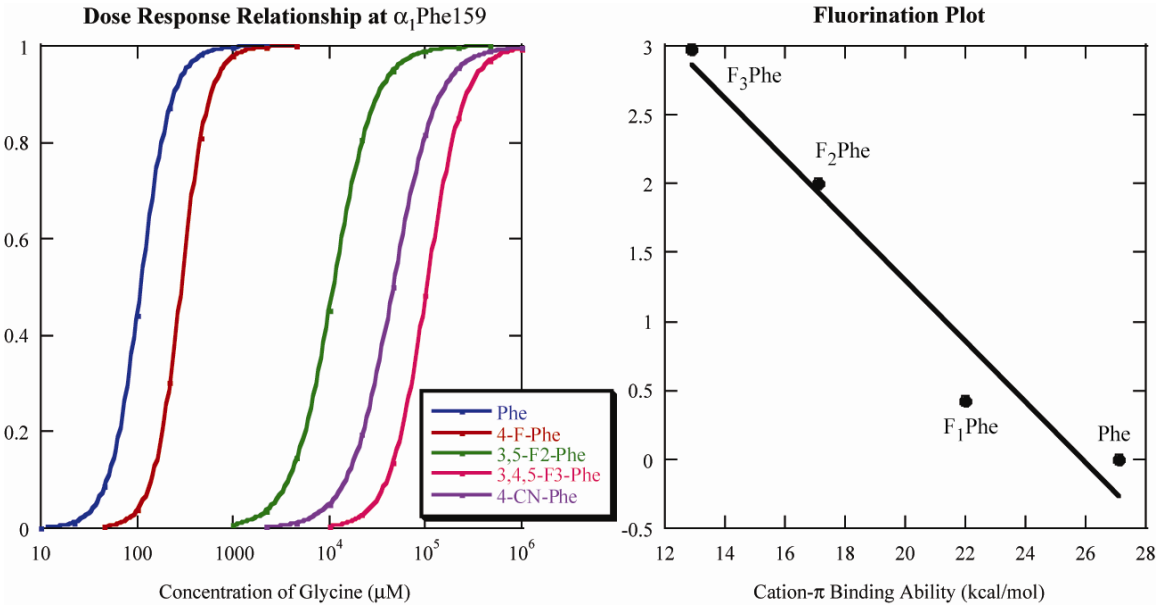

Figure 5.5 The dose response relationship shifts right indicating loss-of-funtion with addition of fluorine residues (left panel). The fluorination plot (right panel) for Phe and Phe analogs at Phe159 in α_1 GlyR

The addition of a single fluorine at Phe207 (F_1Phe) resulted in no change in the glycine EC_{50} value (Table 5.5). However, the addition of larger groups, methyl, methoxy, and cyano, at the 4 position yielded EC_{50} values 10- to 30-fold higher. Incorporation of 3,5-F_2Phe and 3,4,5-F_3Phe increased EC_{50} 500-fold and 100-fold, respectively. These results are not consistent with a cation-π interaction involving Phe207.

Table 5.5 EC_{50} values (μM) for incorporation of fluorinated Phe residues at Phe207 (green, left) and for simultaneous incorporation at Phe159 and Phe207 (red, right). I_{max} is reported in μA.

Amino Acid	EC_{50}	n_H	I_{max}	N	Amino Acid	EC_{50}	n_H	I_{max}	N
Phe	114	2.2	11 ± 1	4	Phe	131	2.7	9 ± 1	18
F_1Phe	151	2.4	10 ± 3	4	F_1Phe	287	2.6	8 ± 2	13
F_2Phe	56700	2.4	8.1 ± 0.2	5	CN-Phe	>400000	1.7	7.4 ± 0.7	4
F_3Phe	13500	2.4	8 ± 1	8					
CN-Phe	3910	2.6	10 ± 1	4					
Me-Phe	1020	2.2	10 ± 3	4					
OMe-Phe	2520	2.2	10 ± 0.4	4					

Additional evidence against a cation-π interaction at Phe 207 stems from results with the Phe159TAG/Phe207TAG double mutant receptor (Table 5.5). If Phe159 and Phe207 both contribute to a cation-π interaction with the glycine amine group, a large increase in EC_{50} would be expected when both interactions are simultaneously weakened. Receptors containing the Phe159TAG/Phe207TAG mutation displayed robust expression and electrophysiological properties similar to those of wild-type receptors when coinjected with Phe-tRNA. Addition of a single fluorine (4-F_1Phe) to both sites produced receptors with only a small decrease in glycine sensitivity (Table 5.5). The Phe159TAG/Phe207TAG double mutant did not produce a functional receptor with 3,5-F_2Phe-tRNA. However, introduction of a cyano group (4-CN-Phe) yielded receptors displaying a greatly reduced glycine sensitivity, with an EC_{50} value in excess of 400 mM.

Table 5.6 EC_{50} values (μM) for incorporation of fluorinated Phe residues at Phe63. I_{max} is reported in μA.

Amino Acid	EC_{50}	n_H	I_{max}	N	Amino Acid	EC_{50}	n_H	I_{max}	N
Phe	113	2.6	9 ± 1	7					
4-F_1Phe	34.5	2.8	8.9 ± 0.7	7	4-CN-Phe	6.5	2.7	8 ± 2	5
3,5-F_2Phe	210	2.1	3 ± 1	3	3,4,5-F_3Phe	348	2.8	4.2 ± 0.7	5

Introduction of a single fluorine in the 4 position at Phe63 decreased the EC_{50} value by a factor of three (Table 5.6). Substitution with 3,5-F_2Phe or 3,4,5-F_3Phe caused relatively small (2- to 3-fold) changes in EC_{50} value that produced no consistent trend when combined with F_1Phe data. We note that 3,5-F_2Phe and 3,4,5-F_3Phe produced significantly lower maximal currents, which may inflate the EC_{50} values slightly.[15] To ensure the lower maximal currents were not causing substantial artifacts in the data, we also incorporated 4-CN-Phe which gave maximal currents similar to both Phe and 4-F_1Phe. Cyano is strongly deactivating in a cation-π interaction (Figure 5.3),[4] and its introduction at a site where a cation-π interaction is present will substantially increase EC_{50}. Mutation to 4-CN-Phe substantially *decreased* EC_{50}, confirming that Phe63 does not participate in a cation-π interaction.

5.3 Discussion

5.3.1 A Cation-π Interaction at Loop A of $GABA_AR$

The $GABA_A$ receptor binding site has been intensively investigated using a range of techniques, including mutagenesis, radioligand binding assays, and photoaffinity labeling.[16-20] These techniques have implicated many amino acids that may be important in the binding site, but they cannot identify the chemical-scale interactions of each amino acid with the neurotransmitter. Here, we used unnatural amino acid mutagenesis combined with functional studies to probe the effects of subtle chemical modifications to aromatic amino acids that form a critical part of this binding site. The results indicate that β_2Tyr97 contributes to a cation-π interaction, the hydroxyl groups of β_2Tyr157 and β_2Tyr205 are critical to receptor function, and that α_1Phe65 is insensitive to subtle chemical changes.

Cysteine accessibility studies previously showed that β_2Tyr97Cys is protected from covalent modification by the presence of GABA or the $GABA_A$ receptor antagonist gabazine (SR95531).[20] indicating this residue lies in the binding pocket of the receptor. Furthermore, mutation to Cys had the same ~100-fold increase on the GABA EC_{50} and on the SR95531 IC_{50}. EC_{50} is an equilibrium measure which incorporates both binding events (the on and off rate of the agonist) and channel activation (the opening and closing rate), thus changes in EC_{50} cannot be directly attributed to changes in the agonist affinity. The antagonist, SR95531, is not able to activate the $GABA_AR$, thus the IC_{50} (concentration of antagonist necessary to achieve half maximal inhibition) is dependent only on binding events. Similar shifts in the EC_{50} of GABA and IC_{50} of SR95531 for the β_2Tyr97Cys mutant strongly indicate that changes in EC_{50} resulting from mutation of β_2Tyr97 are the result of changes in GABA binding.

Our data show a strong correlation between the cation-π binding ability of tyrosine derivatives incorporated at $\beta_2$97 and the EC_{50} (Figure 5.4). The size of this effect and the systematic dependence on the number of fluorines unambiguously establish a cation-π interaction at this site.

The fluorination plot indicates that β_2Tyr97 is involved in a cation-π interaction but does not indicate that the cationic partner is GABA. There are four positively charged amino acids within 10Å of β_2Tyr97 that could perform this role, and without detailed structural information it is difficult to exclude these residues. A homology model of the $GABA_AR$[21] indicates the β_2Lys102 and β_2Lys103 side chains face away from the binding site, suggesting they are unlikely partners for the cation-π interaction.

α_1Arg132 is positioned such that it could interact with β_2Tyr97 but this interaction would restructure the aromatic box such that GABA would not access the binding site. β_2Arg207, the remaining positively charged residue, has previously been proposed to interact with the carboxylate of GABA[22] and would therefore exclude it from contributing to a cation-π interaction at the other end of the molecule. Because all full GABA agonists have a charged amine, it is not possible to use an alternative agonist to provide definitive proof, but given the arguments described above, combined with the precedence of the ligand as the source of the cation in other Cys-loop receptors, we believe that GABA is the source of the cation.

Table 5.7 Sequence Alignment of loop A in the principle subunit of Cys-loop receptor binding sites

Subunit	Alignment	Alternate Alignment
AChBP	SSL**W**V**PD**LAA**Y**-**N**-AISK	SSL**W**V**PD**LAA**Y**-**N**-AISK
nACh α_1	ERI**W**R**PD**LVL**Y**-**N**NADGD	ERI**W**R**PD**LVL**Y**-**N**NADGD
5-HT_{3A}	DSI**W**V**PD**ILI-**N**EFVDVG	DSI**W**V**PD**ILI-**N**EFVDVG
Gly α_1	DSI**W**K**PD**LFFA-**N**EKGAH	DSI**W**K**PD**L--FFA-**N**EKG
$GABA_C$ ρ_1	KKI**W**V**PD**MFFVHSKRSF	KKI**W**V**PD**--MFFVHSKR
$GABA_A$ β_2	DQL**W**V**PD**TYFL-**N**DKKSF	DQL**W**V**PD**--TYFL-**N**DKK

The conserved WxPDxxxxN are shown in bold. The loop A residue of the aromatic box is highlighted.

Thus, the $GABA_A$ receptor becomes the first instance of a Cys-loop receptor that displays a cation-π interaction with a loop A residue. Loop A does contain an aromatic box residue in the nACh receptor, αTyr93, and in the AChBP crystal structures this Tyr aligns with Tyr89, which is clearly located at the "bottom" of the aromatic box. Presumably, $\beta_2$97 of the $GABA_A$ receptor plays the role of αTyr93 and Tyr89, but the alignment is problematic; a gap equivalent to 2 amino acids is required to bring the $\beta_2$97 into alignment with the nACh receptor and AChBP tyrosine residues (Table 5.7). Loop A contains a highly conserved WxPDxxxxN motif, which plays a crucial role in

positioning the rest of the binding site, particularly loop B.[23,24] It is therefore surprising that a gap insertion is necessary in a conserved region with such an important structural role, but the mutagenesis results are compelling.

The location of a cation-π interaction on loop A, contrasting to loop B for other members of the Cys-loop family, supports previous suggestions that a "lock-and-key" metaphor is not appropriate for such receptors.[7] If they required a precise protein–ligand lock-and-key interaction, we would expect related receptors to use cation-π interactions at a conserved location in the three-dimensional structure. This is not the case in the 5-HT-gated 5-HT_3 and MOD-1 receptors, in which the cation-π interactions occur on loop B and loop C, respectively.[5,7] We now find similar variability in the ionotropic GABA receptor family; the cation-π interaction moves from loop B in the $GABA_CR$[8] to loop A in the $GABA_AR$ (the present study). These are very similar receptors, showing 39% sequence identity and 64% homology between $GABA_A(\beta_2)$ and $GABA_C(\rho_1)$ in the extracellular domain. Nevertheless, GABA binds with different orientations in the two receptors. Apparently Cys-loop receptors require only that a ligand occupies the general binding region defined approximately by the aromatic box.

There is no cation-π interaction at $\alpha_1$65: addition of 4-F to the phenyl ring increased GABA EC_{50} slightly, but addition of more fluorines around the ring resulted in no additional increase. This residue has been previously reported to play a role in GABA binding: mutation of α_1Phe64 (α_1Phe65 by human numbering) to Leu increased the GABA EC_{50} from 6 to 1260 μM, with the IC_{50} values of bicuculline and SR95531 increasing by similar amounts.[16] This suggests that the effects of mutations at this position are attributable to disruption of binding rather than gating, and that an aromatic

is preferred here, although our data indicate that α_1Phe65 is tolerant to small chemical changes. A model of the $GABA_AR$[21] indicates that α_1Phe65 is located on the "right-hand" face of the aromatic box (Figure 5.2B), and is partially obscured by β_2Tyr157. Taken together, these data and the model suggest that α_1Phe65 contributes to the general hydrophobicity of the region.

Previous data suggest that β_2Tyr157 and β_2Tyr205 specifically participate in GABA binding: phenylalanine mutations at both these sites significantly increased EC_{50} values, whereas activation of the receptors using pentobarbital, which binds at a location distinct from the GABA binding site, resulted in no change in functional response.[17] Similarly, we observed that removal of the OH (introducing Phe) is highly deleterious at both β_2Tyr157 and β_2Tyr205, resulting in ~400- or 24-fold increases in EC_{50}, respectively. Wild-type behavior can be rescued at β_2Tyr157 by incorporation of 4-F or 4-MeO substituents, whereas 4-Me-Phe or multiply fluorinated phenylalanines increased EC_{50} values 35- to 120-fold. These data suggest that the OH of β_2Tyr157 acts as a hydrogen bond acceptor. The strong penalty for removing the OH and the near wild-type behavior of 4-MeO-Phe support this analysis. In this light, the near wild-type behavior for 4-F-Phe is perhaps surprising. Fluorine is the most electronegative element, and as such it is reluctant to donate a lone pair of electrons to a hydrogen bond donor. As a result, organic fluorine (fluorine bonded to a carbon) hardly ever accepts a hydrogen bond, especially if an alternative, better acceptor can be accessed.[25] Inspection of the region around β_2Tyr157 in a receptor model[21] suggests that there are no alternative hydrogen bond acceptors close to the hydroxyl group within the protein. In such a case, even the very poor acceptor of 4-F-Phe may be better than nothing at all (Phe). The data

for β_2Tyr205 show no clear pattern, although there is an indication that an electronegative atom at position 4 is favored.

5.3.2 A Cation-π Interaction at Loop B of GlyR

A previous model of the GlyR[14] indicated a cation-π interaction involving both Phe159 and Phe207 may exist. In addition to these two residues, there are other aromatic residues in the binding pocket (Phe63, Tyr161, Phe99, Phe100, and Tyr202). We omitted Tyr161 from the present study because the Tyr161Ala was previously shown to function despite a 10-fold loss in glycine sensitivity.[26,27] If this residue was involved in a critical cation-π interaction, it seems unlikely that mutation to Ala would only cause a 10-fold shift in channel function. Phe99 and Phe100 in loop B were omitted for similar reasons, as Ala substitution at these sites results in only small changes to the EC_{50} value.[12] It has been convincingly demonstrated that the hydroxyl group of Tyr202 and not its aromatic character is crucial for agonist binding.[13] Therefore, of the seven residues originally identified, only Phe63, Phe159, and Phe207 were plausible candidates for a cation-π interaction.

The data presented here clearly indicate there is a cation-π interaction with Phe159 and not with Phe207 in the α_1 GlyR. These results are in disagreement with a prior model which proposed a cation-π interaction at both Phe159 and Phe207.[14] We performed experiments with double-mutant receptors (Phe159/Phe207) to confirm there was not a dual cation-π interaction. The measured EC_{50} value of ~300 μM for receptors with 4-F_1Phe at both of these positions is close to the calculated value of ~380 μM that would be expected if the EC_{50} value were simply the product of the two individual

mutations. Substitution with 4-CN-Phe at both sites resulted in functional receptors. Although the glycine EC_{50} value (>400 mM) of the double mutant could not be determined, the data are consistent with the EC_{50} value of ~1.5 M calculated by multiplying the EC_{50} value of the two single mutations. For a dual cation-π interaction we would expect to see an EC_{50} for the double mutant that differed from that predicted by the EC_{50} values of the single mutations. Together, the results from both the Phe207TAG single mutant and the Phe159TAG/Phe207TAG double mutant support the presence of only one cation-π interaction in the GlyR binding site, namely that at position 159.

The data presented here rule out a cation-π interaction at position 207. However, previous studies indicate an aromatic residue at this position is imperative for proper receptor function.[14] Phe207 was highly sensitive to all Phe analogues except 4-F_1Phe, suggesting a sensitivity to the addition of steric bulk, especially at the 3 and 5 positions of the phenyl ring. This result is surprising since a hydrogen to fluorine substitution is usually well tolerated.[3-5,7,8,21,28] Perhaps the higher sensitivity to these mutations in the GlyR is due to the smaller size of the neurotransmitter. Since glycine is a smaller molecule than the ligands that activate other Cys-loop receptors, the GlyR binding site may be more compact than any of the other aromatic boxes examined thus far, thereby making it more sensitive to incorporation of Phe analogues with substituents at the 3 and 5 positions or bulky substituents at the 4 position.

5.3.3 Cys-loop Receptor Cation-π Interactions

A cation-π interaction has been identified in the binding site of all seven cys-loop receptors explicitly tested for the interaction.[3-5,7,8,21,28] Although the location of the interaction varies, the loop B aromatic is involved in five (nAChRs, $5HT_{3A}R$, $GABA_CR$,

and GlyR) of the 7 receptors. The slopes of the fluorination plots are indicative of the strength of the cation-π interaction but (Figure 5.6) vary significantly (3.7-fold) with the $GABA_AR$ having the strongest and the acetylcholine receptors having the weakest. Acetylcholine has a quaternary ammonium group which presents a less focused charge to the aromatic face, thereby decreasing the strength of the cation-π interaction. This may contribute to the shallower slope of the acetylcholine receptors. However, all the other neurotransmitters have primary ammonium moieties, yet there is still a 2.2-fold range in slopes, indicating that the positively charged species alone is not indicative of the strength of the interaction.

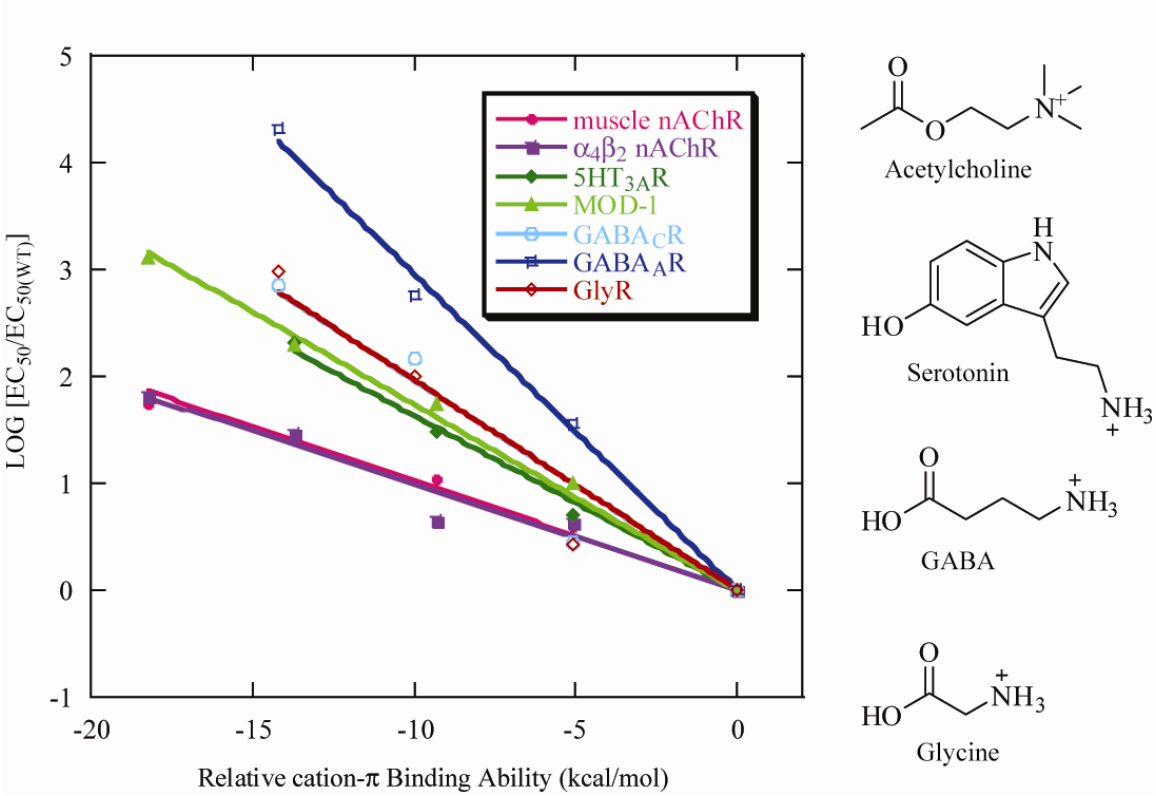

Figure 5.6 Fluorination plot of seven Cys-loop receptors and their neurotransmitter agonists. The $GABA_CR$ (light blue) linear fit is hidden by the GlyR (red).

5.4 Conclusion

In conclusion, cation-π interactions between GABA and a tyrosine on loop A in the $GABA_AR$ and between glycine and a phenylalanine on loop B in the GlyR have been identified by unnatural amino acid mutagenesis. The $GABA_AR$ is the first example of a cation-π interaction with a loop A residue in a Cys-loop receptor, while the cation-π interaction in the GlyR is the first example of such an interaction between a neurotransmitter and phenylalanine residue. The location of the cation-π interaction is not conserved among closely related members of the Cys-loop family, as evidenced by the different locations for the $GABA_A$ (loop A) and $GABA_C$ (loop B) receptors. The results presented here, along with previous studies that identified cation-π interactions in other Cys-loop receptors, emphasize the importance of the cation-π interaction to neurotransmitter binding and thus proper brain function.

5.5 Materials and Methods

Mutagenesis and preparation of mRNA: Mutant $GABA_A$ receptor subunits were developed using pcDNA3.1 (Invitrogen, Abingdon, UK) containing the complete coding sequence for either the human α_1 or human β_2 $GABA_A$ receptor subunit kindly provided by Dr. K. A. Wafford (Merck, Sharp, and Dohme, Harlow, Essex, UK). The codons at positions $\alpha_1$65, $\beta_2$97, $\beta_2$157, and $\beta_2$205 were replaced by a TAG codon as described previously (Beene et al., 2002). Mutagenesis reactions were performed using the method of Kunkel (1985) and confirmed by DNA sequencing. The human GlyR α_1 subunit cDNA was subcloned into pGEMHE to increase expression in oocytes. Site-directed mutagenesis to a TAG codon at positions 63, 159, and 207 was performed with the

QuickChange mutagenesis kit (Stratagene). The mMessage mMachine kit (Ambion) was used to generate capped mRNA for oocyte injection.

Xenopus laevis (Nasco) oocytes were prepared as described below and injected with 5 ng ($GABA_AR$) or 10 ng of mRNA. After injection, oocytes were incubated for 24-48 hours at 18°C prior to electrophysiology recordings.

Xenopus oocyte preparation: Harvested stage V–VI *Xenopus* oocytes were washed in four changes of OR2 buffer (in mM: 82.5 NaCl, 2 KCl, 1 MgCl2, 5 HEPES, pH 7.5), defolliculated in 1 mg/ml collagenase for ~1 hour, washed again in four changes of OR2, and transferred to 70% Leibovitz media (Invitrogen) buffered with 10 mM HEPES, pH 7.5. The following day, they were injected with 5 ng ($GABA_AR$) or 10 ng (GlyR) of mRNA. Electrophysiological measurements were performed 24–72 h after injection.

Synthesis of tRNA and dCA amino acids. This was as described previously (Beene et al., 2004). Briefly, unnatural amino acids were chemically synthesized as nitroveratryloxycarbonyl-protected (NVOC) cyanomethyl esters and coupled to the dinucleotide dCA, which was then enzymatically ligated to 74-mer THG73 $tRNA_{CUA}$ as detailed previously.[10] Immediately before coinjection with mRNA, aminoacyl tRNA was deprotected by photolysis.[29] For the $GABA_AR$ 5 ng of total cRNA was typically injected (1 ng of wild-type α_1 or β_2 subunit and 4 ng of the corresponding α_1 or β_2 mutant subunit) with 25 ng of tRNA-aa in a total volume of 50 nl. For the GlyR, 10 ng of mutant α_1 cRNA and 25 ng of tRNA-aa in a total volume of 50 nl was injected. For a control, cRNA alone and cRNA mixed with dCA-THG_{74} tRNA (no unnatural amino acid

attached) were injected into oocytes. No neurotransmitter-induced currents were detected.

Characterization of mutant receptors: Peak GABA-induced currents were recorded at 22-25°C from individual oocytes using the OpusXpress system (Axon Instruments, Molecular Devices). GABA (Sigma, St. Louis, MO) was stored as 100 mM aliquots at -80°C, diluted in ND96 buffer (in mM: 96 NaCl, 2 KCl, 1 MgCl2, 1.8 CaCl2, 5 HEPES, pH 7.5) and delivered to cells via the automated perfusion system of the OpusXpress. Glass microelectrodes were backfilled with 3 M KCl and had a resistance of 0.5-3.9 MΩ. The holding potential was -60 mV. To determine EC_{50} values, GABA concentration–response data were fitted to the Hill equation (equation 5.1), where I_{max} is the maximal peak current and n is the Hill coefficient.

$$I = \frac{I_{\max}}{1 + EC_{50}/[A]^n} \qquad \textbf{Equation 5.1}$$

5.6 References

(1) Akabas, M. H. *Int Rev Neurobiol* **2004**, *62*, 1-43.
(2) Brejc, K.; van Dijk, W. J.; Klaassen, R. V.; Schuurmans, M.; van Der Oost, J.; Smit, A. B.; Sixma, T. K. *Nature* **2001**, *411*, 269-76.
(3) Xiu, X.; Puskar, N. L.; Shanata, J. A.; Lester, H. A.; Dougherty, D. A. *Nature* **2009**.
(4) Zhong, W.; Gallivan, J. P.; Zhang, Y.; Li, L.; Lester, H. A.; Dougherty, D. A. *Proc Natl Acad Sci U S A* **1998**, *95*, 12088-93.
(5) Beene, D. L.; Brandt, G. S.; Zhong, W.; Zacharias, N. M.; Lester, H. A.; Dougherty, D. A. *Biochemistry* **2002**, *41*, 10262-9.
(6) Beene, D. L.; Price, K. L.; Lester, H. A.; Dougherty, D. A.; Lummis, S. C. *J Neurosci* **2004**, *24*, 9097-104.
(7) Mu, T. W.; Lester, H. A.; Dougherty, D. A. *J Am Chem Soc* **2003**, *125*, 6850-1.
(8) Lummis, S. C.; D, L. B.; Harrison, N. J.; Lester, H. A.; Dougherty, D. A. *Chem Biol* **2005**, *12*, 993-7.
(9) Mecozzi, S.; West, A. P., Jr.; Dougherty, D. A. *Proc Natl Acad Sci U S A* **1996**, *93*, 10566-71.
(10) Nowak, M. W.; Gallivan, J. P.; Silverman, S. K.; Labarca, C. G.; Dougherty, D. A.; Lester, H. A. *Methods Enzymol* **1998**, *293*, 504-29.
(11) Nowak, M. W.; Kearney, P. C.; Sampson, J. R.; Saks, M. E.; Labarca, C. G.; Silverman, S. K.; Zhong, W.; Thorson, J. S.; Abelson, J. N.; Davidson, N.; Schultz, P. G.; Dougherty, D. A.; Lester, H. A. *Science* **1995**, *268*, 439-442.
(12) Vafa, B.; Lewis, T. M.; Cunningham, A. M.; Jacques, P.; Lynch, J. W.; Schofield, P. R. *J Neurochem* **1999**, *73*, 2158-66.
(13) Rajendra, S.; Vandenberg, R. J.; Pierce, K. D.; Cunningham, A. M.; French, P. W.; Barry, P. H.; Schofield, P. R. *EMBO J* **1995**, *14*, 2987-98.
(14) Grudzinska, J.; Schemm, R.; Haeger, S.; Nicke, A.; Schmalzing, G.; Betz, H.; Laube, B. *Neuron* **2005**, *45*, 727-39.
(15) De Saint Jan, D.; David-Watine, B.; Korn, H.; Bregestovski, P. *J Physiol* **2001**, *535*, 741-55.
(16) Sigel, E.; Baur, R.; Kellenberger, S.; Malherbe, P. *EMBO J* **1992**, *11*, 2017-23.
(17) Amin, J.; Weiss, D. S. *Nature* **1993**, *366*, 565-9.
(18) Smith, G. B.; Olsen, R. W. *J Biol Chem* **1994**, *269*, 20380-7.
(19) Boileau, A. J.; Evers, A. R.; Davis, A. F.; Czajkowski, C. *J Neurosci* **1999**, *19*, 4847-54.
(20) Boileau, A. J.; Newell, J. G.; Czajkowski, C. *J Biol Chem* **2002**, *277*, 2931-7.
(21) Padgett, C. L.; Hanek, A. P.; Lester, H. A.; Dougherty, D. A.; Lummis, S. C. *J Neurosci* **2007**, *27*, 886-92.
(22) Wagner, D. A.; Czajkowski, C.; Jones, M. V. *J Neurosci* **2004**, *24*, 2733-41.
(23) Cashin, A. L.; Petersson, E. J.; Lester, H. A.; Dougherty, D. A. *J Am Chem Soc* **2005**, *127*, 350-6.
(24) Lee, W. Y.; Sine, S. M. *J Gen Physiol* **2004**, *124*, 555-67.
(25) Dunitz, J. D. *Chembiochem* **2004**, *5*, 614-21.
(26) Vandenberg, R. J.; French, C. R.; Barry, P. H.; Shine, J.; Schofield, P. R. *Proc Natl Acad Sci U S A* **1992**, *89*, 1765-9.
(27) Yang, Z.; Ney, A.; Cromer, B. A.; Ng, H. L.; Parker, M. W.; Lynch, J. W. *J Neurochem* **2007**, *100*, 758-69.
(28) Pless, S. A.; Millen, K. S.; Hanek, A. P.; Lynch, J. W.; Lester, H. A.; Lummis, S. C.; Dougherty, D. A. *J Neurosci* **2008**, *28*, 10937-42.
(29) Kearney, P. C.; Nowak, M. W.; Zhong, W.; Silverman, S. K.; Lester, H. A.; Dougherty, D. A. *Mol Pharmacol* **1996**, *50*, 1401-12.